Intersymbol and Intercarrier Interference in OFDM Systems: Unified Formulation and Analysis

Fernando Cruz–Roldán, *Senior Member, IEEE,* Wallace A. Martins, *Senior Member, IEEE,*
Fausto García G., Marc Moonen, *Fellow, IEEE*, Paulo S. R. Diniz, *Fellow, IEEE*

Abstract—A unified matrix formulation is presented for the analysis of intersymbol and intercarrier interference in orthogonal frequency-division multiplexing (OFDM) systems. The proposed formulation relies on six parameters and allows studying various schemes, including those with windowing in the transmitter and/or in the receiver (called windowed OFDM systems), which may add cyclic suffix and/or cyclic prefix (CP), besides the conventional CP-OFDM. The proposed framework encompasses seven different OFDM systems. It considers the overlap-and-add procedure performed in the transmitter of windowed OFDM systems, being jointly formulated with the channel convolution. The intersymbol and intercarrier interference, caused when the order of the channel impulse response is higher than the number of CP samples, is characterized. A new equivalent channel matrix that is useful for calculating both the received signal and the interference power is defined and characterized. Unlike previous works, this new channel matrix has no restrictions on the length of the channel impulse response, which means that the study is not constrained to the particular case of two or three data blocks interfering in the received signal. Theoretical expressions for the powers of three different kinds of interference are derived. These expressions allow calculating the signal-to-interference-plus-noise ratio, useful for computing the data rate of each OFDM system. The proposed formulation is applied to realistic examples, showing its effectiveness through comparisons based on numerical performance assessments of the considered OFDM systems.

Index Terms—Orthogonal frequency-division multiplexing (OFDM), windowed orthogonal frequency-division multiplexing (w-OFDM), WOLA-OFDM, cyclic prefix (CP), cyclic suffix (CS), signal-to-interference-plus-noise ratio (SINR).

I. INTRODUCTION

IN MULTICARRIER MODULATION (MCM) systems, frequency-selective communication channels are effectively partitioned into a set of flat-fading channels, whose effects can be equalized by using one coefficient per subcarrier. MCM can be implemented in several ways, but the most popular is orthogonal frequency-division multiplexing (OFDM) [1]–[4].

F. Cruz-Roldán and F. García G. are with the Department of Teoría de la Señal y Comunicaciones, Escuela Politécnica Superior de la Universidad de Alcalá, 28871 Alcalá de Henares (Madrid), Spain (e-mail: fernando.cruz@uah.es).

W.A. Martins and P.S.R. Diniz are with the Electrical Engineering Program (PEE/Coppe) and the Department of Electronics and Computer Engineering (DEL/Poli), Federal University of Rio de Janeiro (UFRJ), 21941-972, Rio de Janeiro/RJ, Brazil (e-mails: {wallace.martins,diniz}@smt.ufrj.br). W.A. Martins is also with the Interdisciplinary Centre for Security, Reliability and Trust (SnT), University of Luxembourg, Luxembourg.

M. Moonen is with the Department of Electrical Engineering (ESAT-STADIUS), KU Leuven, 3001 Leuven, Belgium (e-mail: Marc.Moonen@esat.kuleuven.be).

TABLE I
CHARACTERISTICS OF THE CONSIDERED OFDM SYSTEMS

System	Windowing Side	CP	CS	Example of Reference
CP-OFDM	✗	✓	✗	[2]
wtx-OFDM	Tx	✓	✓	[15]
wrx-OFDM	Rx	✓	✓	[16]
WOLA-OFDM	Tx/Rx	✓	✓	[17]
CPW-OFDM	Tx/Rx	✓	✓	[18]
CPwtx-OFDM	Tx	✓	✗	[7]
CPwrx-OFDM	Rx	✓	✗	[19]

OFDM is based on the discrete Fourier transform (DFT) and offers simplicity and effectiveness against frequency-selective fading, relative insensitivity to timing offsets, compatibility with multiple-input multiple-output (MIMO) systems, and the ability to support multiple access. OFDM is the downlink physical layer modulation scheme of LTE/LTE-A, where it has attained high efficiency for mobile broadband (MBB) services.

In the context of 5G, alternative schemes or waveforms [5], [6] for providing new services were extensively studied, such as massive machine-type communications (mMTC), also known as the Internet of things (IoT), or vehicular to everything (V2X). Among them, windowed OFDM (w-OFDM) has been selected by 3GPP in 5G New Radio (NR) Phase 1. One reason for this selection was that OFDM would not have a severe negative impact on the MBB service, unlike other solutions such as wavelet OFDM or filter-bank multicarrier (FBMC) [7]–[9], which are not fully compatible with the existing OFDM-based solutions.

The w-OFDM is a variation of OFDM that includes pulse-shaping or time-domain windowing. In addition, the windowed parts overlap with each other so as to reduce the time-domain overhead resulting from the windowing, achieving the same spectral efficiency as conventional cyclic-prefix OFDM (CP-OFDM). Due to its smooth transitions in the time domain, w-OFDM reduces side-lobe levels and achieves better spectral efficiency, a higher reduction of the out-of-band (OOB) emission and/or adjacent channel interference (ACI) rejection, compared to conventional CP-OFDM. For these reasons, w-OFDM has been widely deployed in several wireless and wireline communication standards (e.g., see [10]–[14]).

It is possible to find in the literature different w-OFDM systems [2], [5]–[7], [15]–[25]. They comprise time-domain windowing in the transmitter (Tx) (e.g. [15]), which helps to control undesired OOB spectral components, i.e., to reduce

TABLE II
TYPICAL PARAMETERS USED IN THE CONSIDERED OFDM SYSTEMS, FOR A GIVEN ν-ORDER CHANNEL IMPULSE RESPONSE.

Parameter	Description	CP-OFDM	wtx-OFDM	wrx-OFDM	WOLA-OFDM	CPW-OFDM	CPwtx-OFDM	CPwrx-OFDM
μ	CP length	$\mu \geq \nu$	$\mu - \beta \geq \nu$	$\mu - \frac{\delta}{2} \geq \nu$	$\mu - \beta - \delta \geq \nu$	$\mu - \beta - \frac{\delta}{2} \geq \nu$	$\mu - 2\beta \geq \nu$	$\mu - \delta \geq \nu$
β	Tx window tail	0	$\beta < \mu$	0	$\beta < \mu - \delta$	$\beta < \mu - \frac{\delta}{2}$	$\beta < \frac{\mu}{2}$	0
δ	Rx window tail	0	0	$\frac{\delta}{2} \leq \mu$	$\delta \leq \mu - \beta$	$\frac{\delta}{2} \leq \mu - \beta$	0	$\delta \leq \mu$
ρ	CS length	0	β	$\frac{\delta}{2}$	β	$\beta + \frac{\delta}{2}$	0	0
γ	Rx removed samples	μ	μ	$\mu - \frac{\delta}{2}$	$\mu - \delta$	$\mu - \frac{\delta}{2}$	$\mu - \beta$	$\mu - \delta$
κ	Rx circular shift	0	0	0	$\frac{\delta}{2}$	0	β	$\frac{\delta}{2}$

spectral leakage. Some systems also include a time-domain windowing in the receiver (Rx) to increase the OOB rejection and to reduce the power of interfering signals [2], [16], [20], [25], which can increase the signal-to-interference-plus-noise ratio (SINR). On the other hand, a CP is always inserted in each transmitted data vector, and in some systems, an additional guard interval or cyclic suffix (CS) is also appended [6], [16]–[18].

In this paper, we focus our attention on the seven OFDM systems shown in Table I. The typical parameter values of each system are given in detail in Table II, and the characteristics of the windows are given in Figs. 1 and 2, where N is the number of subcarriers. First, we include in our study conventional CP-OFDM because the proposed unified formulation is also valid for the most widely standardized MCM scheme. Second, we analyze Tx and Rx time-domain w-OFDM [2], [19], [21], [22], [24], respectively referred to as wtx-OFDM and wrx-OFDM. Third, our study also includes the weighted overlap-and-add OFDM (WOLA-OFDM), proposed for asynchronous 5G [5], [6], [17], also with an additionally extended suffix scheme named CPW-OFDM [18]. As can be seen in Table I, these transceivers use independent time-domain windows in both transmitter and receiver sides, and both CP and CS are inserted into each data vector to be transmitted. Lastly, as there are standards that employ in their physical layers w-OFDM without CS, e.g., [11]–[13], it is necessary to study a fourth group of OFDM systems: they just include CP with a windowing in the Tx (referred to as CPwtx-OFDM) and a windowing in the Rx (CPwrx-OFDM) [7], [23]. Thus, our study covers a wide range of w-OFDM systems that will play an important role in various communication systems over the next decade.

OFDM systems suffer from intersymbol and intercarrier interference (ISI and ICI) when the order of the channel impulse response (CIR) does not satisfy the conditions related to the CP length in Table II. In this context, the interference analysis in conventional CP-OFDM has been widely addressed. For instance, different SINR models are derived in [26]–[34]. For more details, we refer the reader to [35], where the impact of highly dispersive channels on OFDM under finite-duration CIR with arbitrary length is shown. Regarding w-OFDM, previous studies focusing on the analysis of interference are [7], [15], [23], [25], [36]. In [7], [15], [23], both ISI and ICI are grouped under a single time-domain term, and the systems analyzed in these papers are CPwtx-OFDM [7], [15], [23] with a unique windowing in the Tx unit, and wtx-OFDM [15]. In [25], an Rx windowing OFDM system is
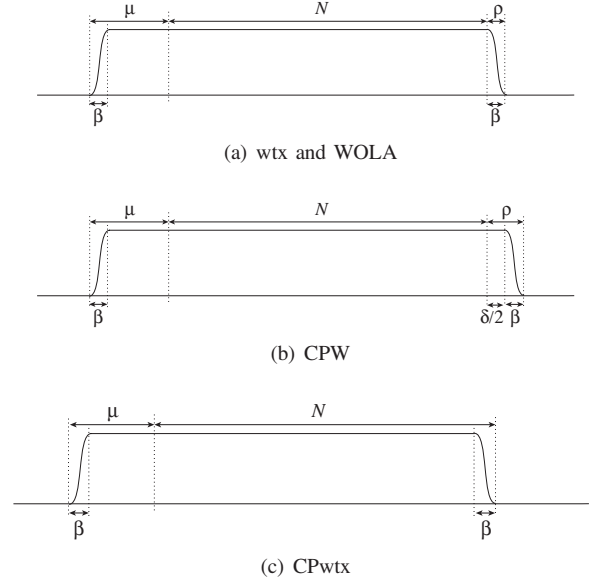

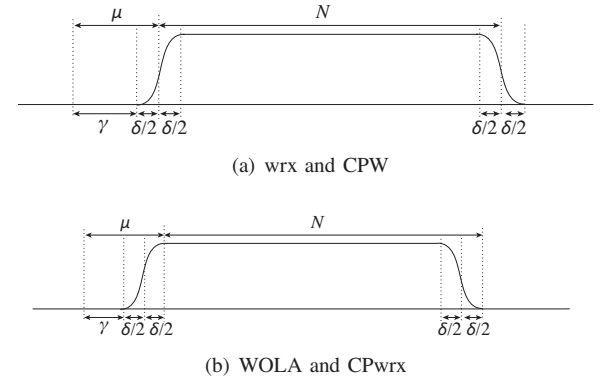Fig. 1. Tx windows: (a) wtx and WOLA, (b) CPW, and (c) CPwtx.

Fig. 2. Rx windows: (a) wrx and CPW, (b) WOLA and CPwrx.

considered, and the ICI induced by the proposed windowing is obtained.

We perform an exhaustive analysis of ICI and ISI in the seven different system considered in our study. Since no constraint is imposed upon the order of the CIR, our results is applicable to the cases where the interference is due to any number of transmitted data blocks. The main contributions in this paper can be summarized as follows:

- A unified matrix formulation for a wide range of OFDM systems is presented. It includes the full transmission

chain, the overlap-and-add operation, the convolution with a channel of arbitrary length, and the reception process. This matrix formulation is a powerful tool to reduce the computational time needed to perform Monte Carlo simulations. Moreover, this compact formulation based on a small set of only six parameters allows easy reconfiguration of the systems —different OFDM systems are obtained by simply changing parameters in the formulation. In addition, it has excellent potential for use in an educational context, because it enables quickly explaining several OFDM systems.

- Theoretical closed-form expressions of interference and noise for the case of an insufficient length of redundant samples (i.e. CP) are obtained. The interference is identified in the frequency domain, where the symbol is reconstructed, and classified into three different classes. This classification helps to study which one is most harmful to the system's performance.
- Interference and noise powers are derived to obtain the SINR, and hence the data rate and the bit-error rate. The results are also useful for bit-loading, adaptive CP and power/subcarrier allocation algorithms [3].

The rest of this paper is organized as follows. In Section II, we present the unified system model, considering seven different OFDM systems and adopting a unified matrix formulation covering all of them. Then, three types of interference are calculated in Section III. In addition, theoretical expressions for both interference and noise powers are derived, and the corresponding SINR is determined. Simulation results are presented in Section IV, and finally, conclusions are drawn in Section V.

The notation used in this paper is as follows. Bold-face letters indicate vectors (lower case) and matrices (upper case). The transpose of $\mathbf{A}$ is denoted by $\mathbf{A}^T$ and $\mathbf{I}_N$ represents the $N \times N$ identity matrix. The subscript is omitted whenever the size is clear from the context. $\mathbf{0}$ and $\mathbf{1}$ denote, respectively, a matrix of zeros or ones.

II. UNIFIED SYSTEM MODEL

A block diagram is shown in Fig. 3, where the transmitted data vector in the transform domain is given by

$$\mathbf{X} = \begin{bmatrix} X_0 & X_1 & \cdots & X_{N-1} \end{bmatrix}^T, \tag{1}$$

with N being the number of subcarriers. The parameters used in the equations are given in detail in Table II. We assume perfect synchronization in time and frequency, and also that the receiver has perfect channel-state information (CSI).

A. Transmitter

The time-domain vector before the overlap-and-add block is

$$\mathbf{x}^{\mathrm{s}}_{(N+\mu+\rho)\times 1} = \mathbf{V}^{\mathrm{tx}}_{(N+\mu+\rho)} \cdot \mathbf{\Gamma}_{(N+\mu+\rho)\times N} \cdot \mathbf{W}^{-1}_N \cdot \mathbf{X}_{N\times 1}.$$

Here, $\mathbf{W}^{-1}$ represents the inverse DFT matrix with the (k,n)-th entry given by

$$\left[\mathbf{W}^{-1}\right]_{k,n} = \frac{1}{N}\mathrm{e}^{\mathrm{j}\frac{2\pi}{N}kn}, \quad 0 \le k,n \le N-1.$$

The matrix $\mathbf{\Gamma}$ introduces $\mu + \rho$ redundant samples:

$$\mathbf{\Gamma} = \begin{bmatrix} \mathbf{0}_{\mu\times(N-\mu)} & \mathbf{I}_\mu \\ \mathbf{I}_N \\ \mathbf{I}_\rho & \mathbf{0}_{\rho\times(N-\rho)} \end{bmatrix}.$$

It appends a μ-length CP and, when applicable, also a ρ-length CS. Observe that a cyclic shift, as employed in [14], is equivalent to the inclusion of a CS into each data vector. The following block performs the windowing, and it can be represented as a diagonal matrix

$$\mathbf{V}^{\mathrm{tx}}_{(N+\mu+\rho)} = \mathrm{diag}\left\{\mathbf{v}^{\mathrm{tx}}_{1\times(N+\mu+\rho)}\right\},$$

obtained with a tapering window function, defined as

$$\mathbf{v}^{\mathrm{tx}}_{1\times(N+\mu+\rho)} = \begin{bmatrix} \mathbf{v}^{\mathrm{tr}}_{1\times\beta} & \mathbf{1}_{1\times(N+\mu+\rho-2\beta)} & \mathbf{v}^{\mathrm{tf}}_{1\times\beta} \end{bmatrix}.$$

The vectors $\mathbf{v}^{\mathrm{tr}}_{1\times\beta}$ and $\mathbf{v}^{\mathrm{tf}}_{1\times\beta}$ have as entries the rise and fall samples of the window tails, respectively.

After the pulse shaping or windowing, there is a β-samples overlap-and-add operation between successive symbols. This operation is jointly formulated with the channel convolution.

B. Channel

The signal $\mathbf{x}^{\mathrm{s}}$ is convolved with the transmission channel, defined as $\mathbf{h} = \begin{bmatrix} h_0 & h_1 & \cdots & h_\nu \end{bmatrix}$, and becomes contaminated by noise. In general, the number of transmitted data vectors that affect the first $N + \delta + \gamma$ samples of the received data vector is $M + 1$, with

$$M \triangleq \left\lceil \frac{\nu + \beta}{N + \delta + \gamma} \right\rceil, \tag{2}$$

in which $\lceil \cdot \rceil$ represents the ceiling function. Therefore, the l-th received signal vector is given by

$$\mathbf{y}^{\mathrm{r}}_{(N+\delta+\gamma)\times 1}[l]$$
$$= \sum_{m=0}^{M} \mathbf{H}^{(m)}_{(N+\delta+\gamma)\times(N+\mu+\rho)} \cdot \mathbf{x}^{\mathrm{s}}_{(N+\mu+\rho)\times 1}[l-m]$$
$$+ \mathbf{q}_{(N+\delta+\gamma)\times 1}[l],$$

where $\mathbf{H}^{(m)}$ is a matrix whose entries, for $0 \le b \le N + \delta + \gamma - 1$ and $0 \le c \le N + \mu + \rho - 1$, are

$$\left[\mathbf{H}^{(m)}\right]_{b,c} \triangleq \begin{cases} 0, & mN_0 + b - c < 0, \\ h_{mN_0+b-c}, & 0 \le mN_0 + b - c \le \nu, \\ 0, & mN_0 + b - c > \nu, \end{cases} \tag{3}$$

where $N_0 = N + \mu + \rho - \beta$ and $\mathbf{q}$ represents the channel noise.

C. w-OFDM Receiver

In the absence of noise, the received data vector can be expressed in the transform domain as

$$\mathbf{Y}_{N\times 1} = \mathbf{W}_N \cdot \mathbf{K}_N \cdot \mathbf{P}_{N\times(N+\delta)} \cdot \mathbf{V}^{\mathrm{rx}}_{(N+\delta)}$$
$$\times \mathbf{R}_{(N+\delta)\times(N+\delta+\gamma)} \cdot \mathbf{y}^{\mathrm{r}}_{(N+\delta+\gamma)\times 1}, \tag{4}$$

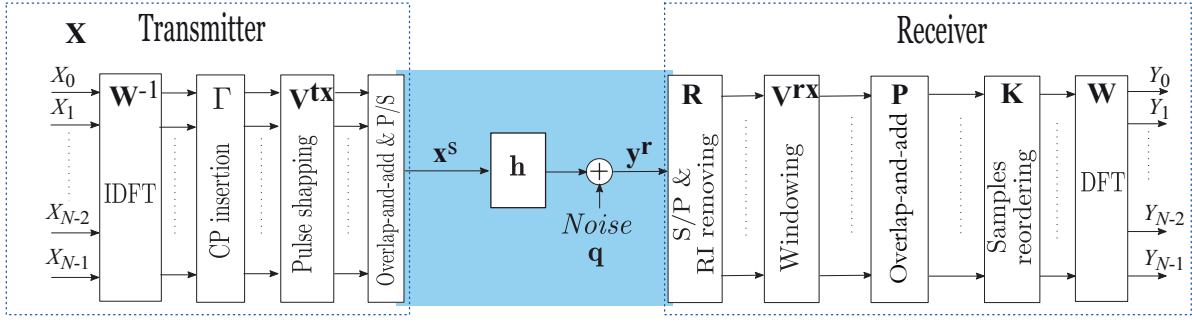where $\mathbf{y}^{\mathrm{r}}_{(N+\delta+\gamma)\times 1}$ is the received signal, and the matrices are defined as follows.

Fig. 3. General block diagram of windowed OFDM over a channel with additive noise.

First, $\mathbf{R}$ represents removal of the first γ samples of the received data vector:

$$\mathbf{R} = \begin{bmatrix} \mathbf{0}_{(N+\delta)\times\gamma} & \mathbf{I}_{(N+\delta)} \end{bmatrix}.$$

The diagonal matrix representing the windowing is

$$\mathbf{V}^{\mathrm{rx}} = \mathrm{diag}\left\{\mathbf{v}^{\mathrm{rx}}_{1\times(N+\delta)}\right\},$$

where the tapering window in the Rx is defined as

$$\mathbf{v}^{\mathrm{rx}} = \begin{bmatrix} \mathbf{v}^{\mathrm{rr}}_{1\times\delta} & \mathbf{1}_{1\times(N-\delta)} & \mathbf{v}^{\mathrm{rf}}_{1\times\delta} \end{bmatrix},$$

where $\mathbf{v}^{\mathrm{rr}}$ and $\mathbf{v}^{\mathrm{rf}}$ have as entries the rise and fall samples of the Rx window tails. Next, $\mathbf{P}$ is a matrix that represents a δ-samples overlap-and-add operation:

$$\mathbf{P} = \begin{bmatrix} \mathbf{0}_{\delta/2} & \mathbf{I}_{\delta/2} & \mathbf{0}_{\delta/2\times(N-\delta)} & \mathbf{0}_{\delta/2} & \mathbf{I}_{\delta/2} \\ & \mathbf{0}_{(N-\delta)\times\delta} & \mathbf{I}_{N-\delta} & \mathbf{0}_{(N-\delta)\times\delta} & \\ \mathbf{I}_{\delta/2} & \mathbf{0}_{\delta/2} & \mathbf{0}_{\delta/2\times(N-\delta)} & \mathbf{I}_{\delta/2} & \mathbf{0}_{\delta/2} \end{bmatrix}.$$

Basically, it adds the first δ samples to the last δ samples. Then, a circular shift of κ samples is needed in some systems (WOLA, CPwtx, and CPwrx). This operation is formulated with the matrix $\mathbf{K}_N$, defined as follows:

$$\mathbf{K}_N = \begin{bmatrix} \mathbf{0}_{(N-\kappa)\times\kappa} & \mathbf{I}_{N-\kappa} \\ \mathbf{I}_\kappa & \mathbf{0}_{\kappa\times(N-\kappa)} \end{bmatrix}.$$

In some other systems, e.g., those that include a CS in each transmitted data vector (wtx and CPW), this is an identity matrix: $\mathbf{K}_N = \mathbf{I}_N$. Finally, $\mathbf{W}$ is a DFT matrix:

$$[\mathbf{W}]_{k,n} = \mathrm{e}^{-\mathrm{j}\frac{2\pi}{N}kn}, \quad 0 \le k, n \le N-1.$$

III. ANALYSIS OF INTERFERENCE

This section provides a comprehensive analysis of the interference and its power for the considered OFDM systems. Given a finite duration CIR with arbitrary length, without any constraint on the length, the received data vector can be expressed in the transform domain as

$$\mathbf{Y}[l] = \sum_{m=0}^{M} \mathbf{A}_m \cdot \mathbf{X}[l-m] + \mathbf{G}^{\mathrm{noise}} \cdot \mathbf{q}[l], \quad (5)$$

where

$$\mathbf{A}_{m,N\times N} = \mathbf{W} \cdot \mathbf{K} \cdot \mathbf{P} \cdot \mathbf{V}^{\mathrm{rx}} \cdot \mathbf{R} \cdot \mathbf{H}^{(m)} \cdot \mathbf{V}^{\mathrm{tx}} \cdot \mathbf{\Gamma} \cdot \mathbf{W}^{-1},$$
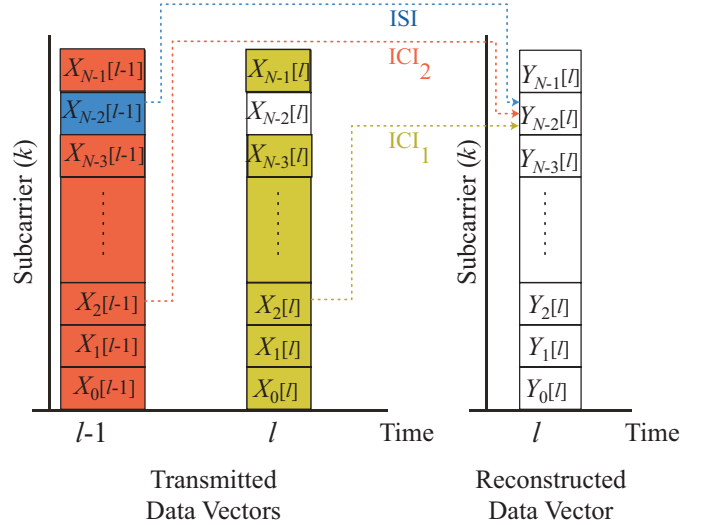

Fig. 4. Types of interference.

$$\mathbf{G}^{\mathrm{noise}}_{N\times(N+\delta+\gamma)} = \mathbf{W} \cdot \mathbf{K} \cdot \mathbf{P} \cdot \mathbf{V}^{\mathrm{rx}} \cdot \mathbf{R}.$$

Note that for $\nu \le \gamma - \beta$, the number of data vectors affecting the reception (in the transform domain) of a single data vector is one. In this case, a set of N independent parallel subcarriers is obtained, each having a channel gain of H_k, defined as the N-point DFT of the CIR $\mathbf{h}$. Thus a one-tap per subcarrier equalizer can be used to mitigate the phase and the amplitude distortion introduced by the channel. This means that $\mathbf{A}_m = 0$, $m > 0$, and $\mathbf{A}_0$ is a diagonal matrix with elements H_k, $0 \le k \le (N-1)$. For the other cases ($\nu > \gamma - \beta$), we have three different types of interference, as depicted in Fig. 4 [35], [37]:

- Type-I intercarrier interference (ICI$_1$): corresponding to the elements $[\mathbf{A}_0]_{i,j}$, $i \ne j$.
- Type-II intercarrier interference (ICI$_2$): corresponding to the elements $[\mathbf{A}_m]_{i,j}$, $i \ne j$, $m > 0$.
- Intersymbol interference (ISI): corresponding to the diagonal elements $[\mathbf{A}_m]_{i,i}$, $m > 0$.

We now derive theoretical expressions for the powers corresponding to the desired signal component in the received data vector, as well as to the ISI, ICI, and noise. These powers are used to compute the SINR. For this study, we assume that the components of the data vector X_k and the noise vector q_k are zero-mean wide-sense stationary uncorrelated processes,

independent and identically distributed for all k, with variances σ_X^2 and σ_n^2, respectively. We follow the same reasoning as in [35]. The desired signal component in the received data vector can be written as

$$\mathbf{Y}_{\text{des}}[l] = \mathbf{A}_0^{\text{des}} \cdot \mathbf{X}[l], \tag{6}$$

where $\mathbf{A}_0^{\text{des}}$ is a diagonal matrix with entries

$$\left[\mathbf{A}_0^{\text{des}}\right]_{i,i} = [\mathbf{A}_0]_{i,i}. \tag{7}$$

The desired signal power (before the transform-domain equalization) at subcarrier k is obtained as the (k, k)-th element of the covariance matrix, i.e., $P_{\text{signal}}(k) = [\mathbf{C}^s]_{k,k}$, where

$$\begin{aligned}
\mathbf{C}^s &= E\left\{\mathbf{Y}_{\text{des}}[l] \cdot \mathbf{Y}_{\text{des}}^H[l]\right\} \\
&= E\left\{\mathbf{A}_0^{\text{des}} \cdot \mathbf{X}[l] \cdot \mathbf{X}^H[l] \cdot \left(\mathbf{A}_0^{\text{des}}\right)^H\right\} \\
&= \mathbf{A}_0^{\text{des}} \cdot E\left\{\mathbf{X}[l] \cdot \mathbf{X}^H[l]\right\} \cdot \left(\mathbf{A}_0^{\text{des}}\right)^H. \\
&= \sigma_X^2 \cdot \mathbf{A}_0^{\text{des}} \cdot \left(\mathbf{A}_0^{\text{des}}\right)^H, \tag{8}
\end{aligned}$$

where $E\{\cdot\}$ is the expected-value operator. The noise data vector is given by

$$\mathbf{Y}_{\text{noise}}[l] = \mathbf{G}^{\text{noise}} \cdot \mathbf{q}[l], \tag{9}$$

As a result, the noise power is given by $P_{\text{noise}}(k) = [\mathbf{C}^n]_{k,k}$, where

$$\mathbf{C}^n = \sigma_n^2 \cdot \mathbf{G}^{\text{noise}} \cdot \left(\mathbf{G}_k^{\text{noise}}\right)^H. \tag{10}$$

The interference component is given by

$$\begin{aligned}
\mathbf{Y}_{\text{int}}[l] &= \mathbf{Y}[l] - \mathbf{Y}_{\text{des}}[l] - \mathbf{Y}_{\text{noise}}[l] \\
&= \mathbf{A}_0^{\text{ICI}_1} \cdot \mathbf{X}[l] + \sum_{m=1}^M \mathbf{A}_m \cdot \mathbf{X}[l-m], \tag{11}
\end{aligned}$$

where $\mathbf{A}_0^{\text{ICI}_1} = \mathbf{A}_0 - \mathbf{A}_0^{\text{des}}$. Using the above, the ISI and ICI power is $P_{\text{ISI,ICI}}(k) = [\mathbf{C}^i]_{k,k}$, where

$$\begin{aligned}
\mathbf{C}^i &= E\left\{\mathbf{Y}_{\text{int}}[l] \cdot \mathbf{Y}_{\text{int}}^H[l]\right\} \\
&= E\left\{\mathbf{A}_0^{\text{ICI}_1} \cdot \mathbf{X}[l] \cdot \mathbf{X}^H[l] \cdot \left(\mathbf{A}_0^{\text{ICI}_1}\right)^H\right\} \\
&\quad + \sum_{m=1}^M E\left\{\mathbf{A}_m \cdot \mathbf{X}[l-m] \cdot \mathbf{X}^H[l-m] \cdot (\mathbf{A}_m)^H\right\} \\
&= \sigma_X^2 \cdot \left(\mathbf{A}_0^{\text{ICI}_1} \cdot \left(\mathbf{A}_0^{\text{ICI}_1}\right)^H + \sum_{m=1}^M \mathbf{A}_m \cdot (\mathbf{A}_m)^H\right). \tag{12}
\end{aligned}$$

Hence, the SINR for subcarrier k is

$$\text{SINR}(k) = \frac{P_{\text{signal}}(k)}{P_{\text{ISI,ICI}}(k) + P_{\text{noise}}(k)}. \tag{13}$$
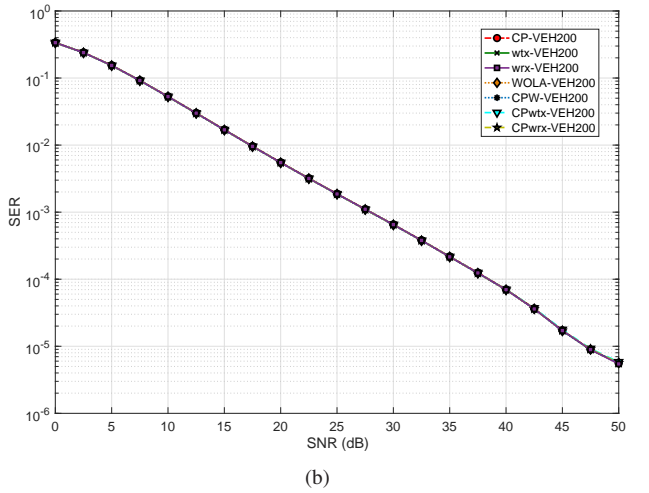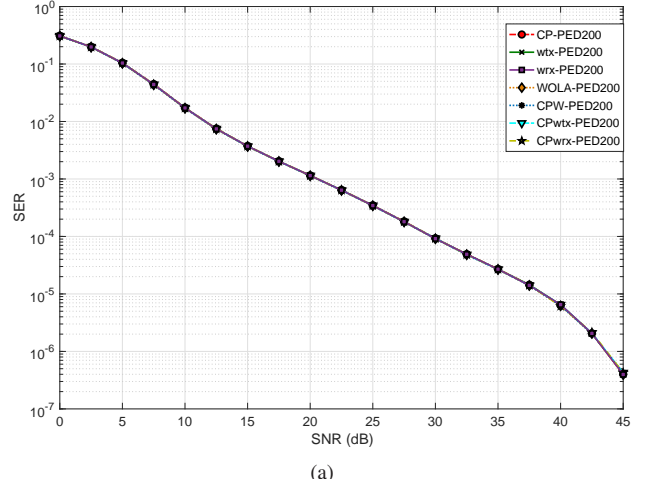

(a)

(b)

Fig. 5. SER versus SNR for different OFDM systems. (a) PED200. (b) VEH200.

IV. SIMULATIONS

In order to demonstrate the applicability of the proposed formulation, this section compares the performance of the studied systems in terms of SER and achievable data rate. It is worth noting that OOB emissions will not be taken into account here. The set of parameters used in the simulations are summarized in Table III. BPSK modulation is used as the primary mapping, the number of active subcarriers is $N = 256$, which is the DFT size, and the frequency spacing is 11.16071492 kHz. Two sets of 250 wireless fading channels each, according to the ITU Pedestrian A and Vehicular A channels [38], [39], are used as multipath channels. They have been generated with Matlab's `stdchan` using the channel models `itur3GPAx` and `itur3GVAx` with a carrier frequency $f_c = 2$ GHz and two different sets of parameters: (a) 4 km per hour as pedestrian velocity, $T_s = 200$ ns and length $L = \nu + 1 = 11$; (b) 100 km per hour as mobile speed, $T_s = 200$ ns and length $L = \nu + 1 = 21$. These channels are referred to as PED200 and VEH200, respectively. The noise is modeled as an additive white Gaussian noise. It is assumed that the channel remains unchanged within the same simulation and perfect channel estimation is performed at the

TABLE III
PARAMETERS USED IN THE EXPERIMENTS ($N = 256$)

Parameter	CP-OFDM	wtx-OFDM	wrx-OFDM	WOLA-OFDM	CPW-OFDM	CPwtx-OFDM	CPwrx-OFDM
β	0	8	0	8	8	8	0
δ	0	0	10	10	10	0	10
ρ	0	8	5	8	13	0	0
γ	32	32	27	22	27	24	22
κ	0	0	0	5	0	8	5

(a)

(b)
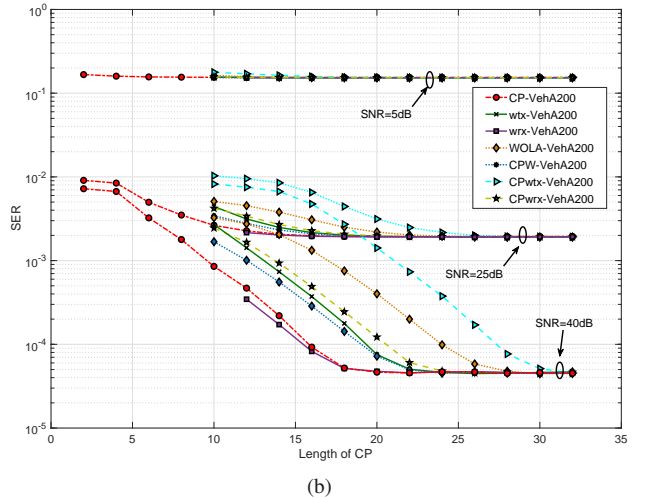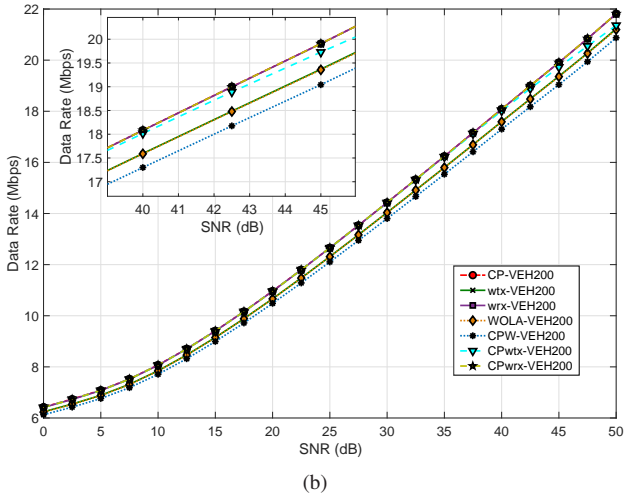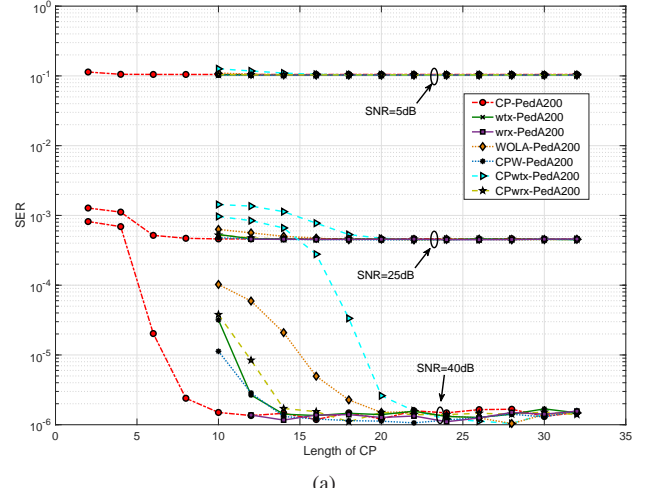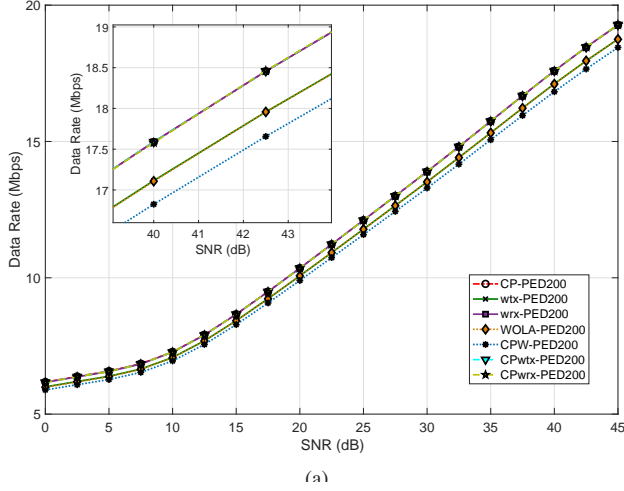
Fig. 6. Total achievable data rate versus SNR for different OFDM systems. (a) PED200. (b) VEH200.

(a)

(b)

Fig. 7. SER versus CP length for different OFDM systems. (a) PED200. (b) VEH200.

receiver. Perfect time and frequency synchronization is also assumed.

In Fig. 5, the symbol error rate (SER) performance curves of the different OFDM systems and channels are depicted. As can be seen, the results for the different systems are practically indistinguishable for each set of channels. Thus, there is no clear advantage in terms of SER of any particular OFDM system over the other systems.

Next, we investigate the data rate performance for a fixed CP length ($\mu = 32$). As we use BPSK modulation, the data rate for subcarrier k is given by [40]

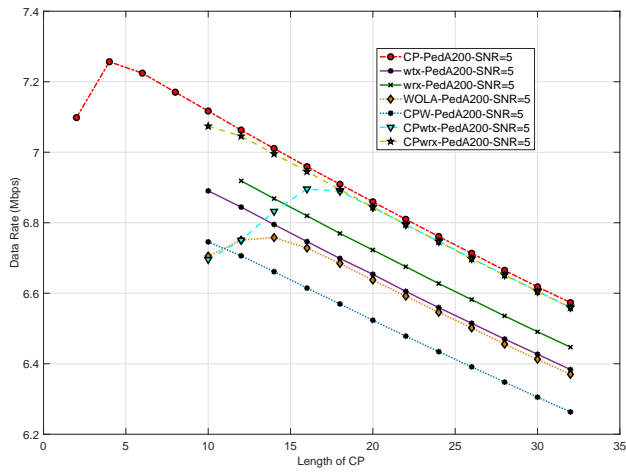$$C(k) = \frac{1}{2} \log_2 \left(\frac{\mathrm{SINR}(k)}{\gamma^*} \right), \qquad (14)$$

where γ^* is the modified SINR gap defined for a target SER as

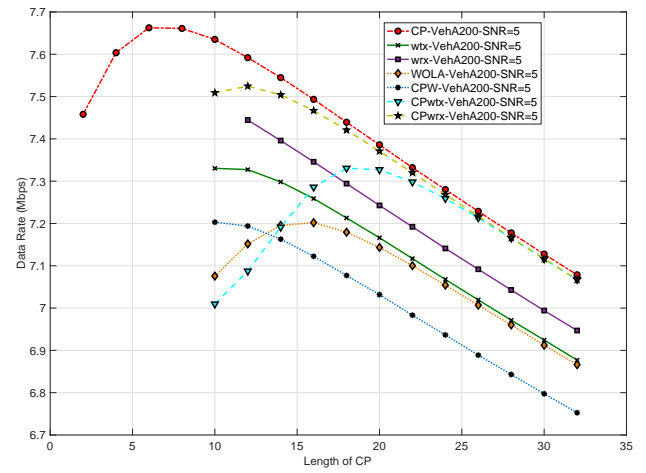$$\gamma^* = \left(\frac{Q^{-1}(\mathrm{SER}/2)}{\sqrt{2}\pi} \right)^2.$$

The total achievable data rate is thus

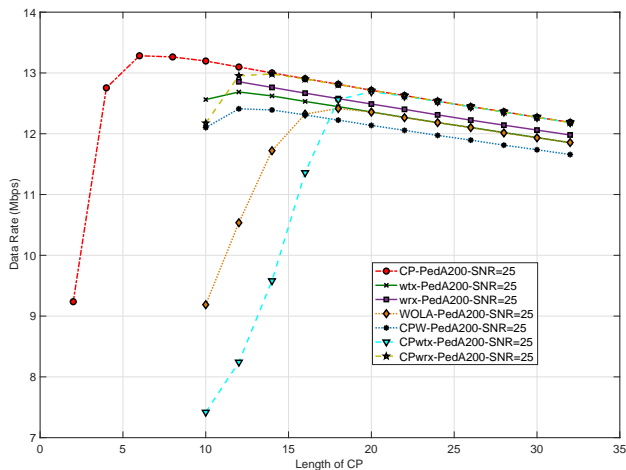$$R = f_\mathrm{s} \sum_{k=0}^{N-1} \frac{N}{N_0} \cdot C(k), \qquad (15)$$

where $N_0 = N + \mu + \rho$ and $f_\mathrm{s} = 1/T_\mathrm{s}$. We employ the SER obtained in the previous simulations to compute the values of γ^* corresponding to each SNR. Fig. 6 shows the resulting data rate as a function of the SNR. In this set of experiments,
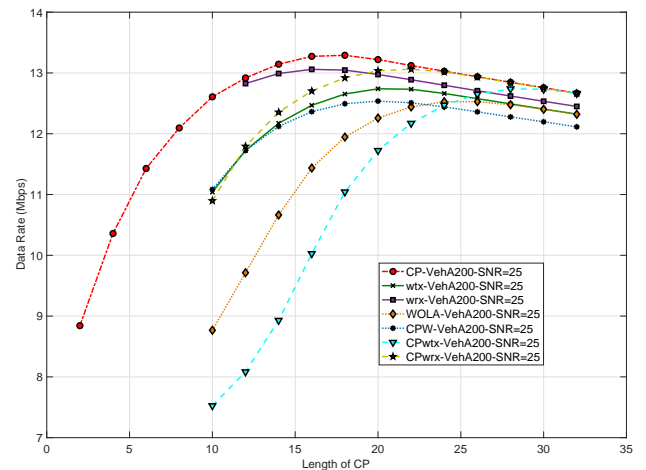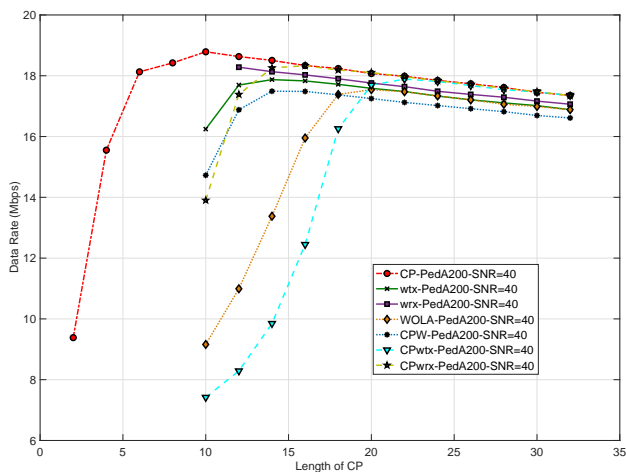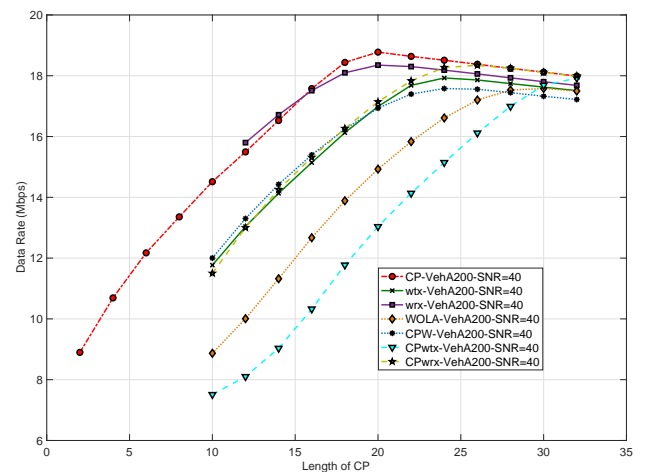
Fig. 8. Achievable data rate for different lengths for the CP and SNR values.
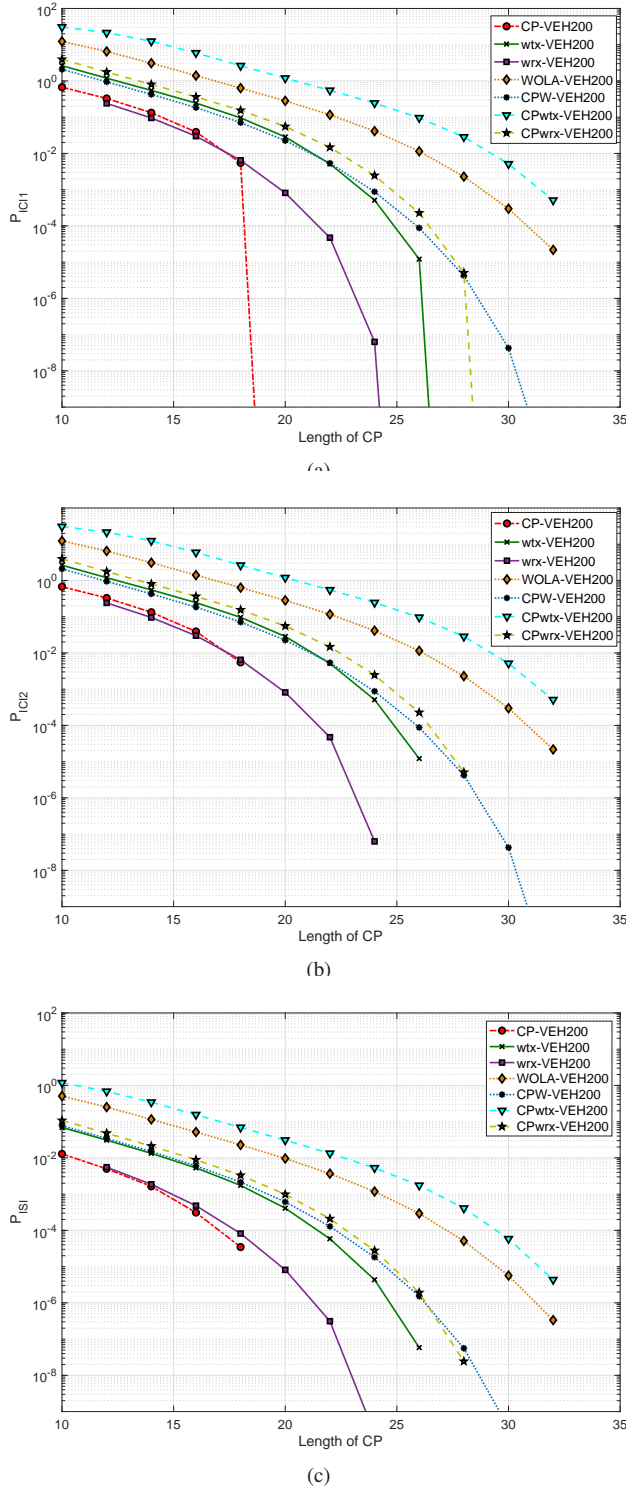
Fig. 9. Total power for different CP lengths. (a) Power of type-I intercarrier interference. (b) Power of type-II intercarrier interference. (c) Power of intersymbol interference.

the OFDM systems that offer the best results are CP, wrx and CPwrx. The systems performing windowing in the receiver and including a prefix and suffix, such as WOLA and CPW, offer a lower transmission rate due to the penalty of adding the two types of redundant samples.

We now analyze the influence of the CP size on the resulting data rate. To this purpose, the SER as a function

of the CP length is obtained for each OFDM system (see Fig. 7), assuming $\mathrm{SNR} = 5, 25,$ and 40 dB. These results are employed to calculate γ^*. Then, we obtain the achievable data rate, depicted in Fig. 8 for the PED200 and VEH200 channels. In all cases, CP-OFDM outperforms the other systems, except for $\mathrm{SNR} = 40$ dB, VEH200, and for smaller values of the CP, for which the wrx scheme shows a better performance. However, this improvement is not very significant in this case of insufficient redundant samples. The remaining OFDM systems have better performance whenever the windowing is in the receiver. For both small CP lengths and low SNR values, the systems that only have a CP outperform those that incorporate a CS.

Finally, the formulation presented here allows analysis in the transform domain of the three different interference powers that appear in each OFDM scheme. Fig. 9 shows the total power results (P_{ICI1}, P_{ICI2}, and P_{ISI}) as a function of the CP length, obtained in the previous experiment for the VEH200 channel. The interference power is higher for systems whose windowing is performed in the transmitter than those with windowing in the receiver. Note that the CPW system has low levels of interference power, but the data rate results do not outperform the other systems. This is due to the overhead involved in the inclusion of both CP and CS.

V. CONCLUSION

In this paper, we presented a unified formulation that describes conventional CP-OFDM and other six different w-OFDM systems. The unified matrix formulation describes the whole transmitter, including the overlap-and-add windowing operation, and the operation of convolving the transmitted signal with the channel, as well as the complete receiver operation. Moreover, we derived expressions for intersymbol interference as well as two different kinds of intercarrier interference, along with their corresponding powers, besides the noise component. We developed analytical expressions for the SINR so as to evaluate the effects of interference on the considered OFDM systems and to study the achievable data rate. Computer simulations were carried out with practical scenarios. Comparing the obtained results, we observed that in terms of SER, all OFDM systems behave similarly. But in terms of data rate criteria, the OFDM systems that only have a windowing in the receiver, or that only include a CP, outperform the others. It has also been noted that some systems (such as CPW-OFDM) have low interference power levels, but the performance in terms of the transmission data rate is slightly lower than other systems with more interference. The reason for this can be found in the penalty paid for including both the prefix and suffix.

REFERENCES

[1] J. A. C. Bingham, "Multicarrier modulation for data transmission: An idea whose time has come," *IEEE Communications Magazine*, vol. 28, no. 5, pp. 5–14, May 1990.

[2] Y.-P. Lin, S.-M. Phoong, and P. P. Vaidyanathan, *Filter Bank Transceivers for OFDM and DMT systems*. Cambridge University Press, 2011.

[3] J. Cioffi, "Digital communications, chap. 4: Multichannel modulation," https://web.stanford.edu/group/cioffi/doc/book/chap4.pdf.

[4] P. S. R. Diniz, W. A. Martins, and M. V. S. Lima, *Block Transceivers: OFDM and Beyond*. Morgan & Claypool, 2012.

[5] X. Zhang, L. Chen, J. Qiu, and J. Abdoli, "On the waveform for 5G," *IEEE Communications Magazine*, vol. 54, no. 11, pp. 74–80, 2016.

[6] "Qualcomm inc. - waveform candidates," Busan, Korea, R1-162199, Apr. 11–15 2016.

[7] P. Achaichia, M. L. Bot, and P. Siohan, "OFDM/OQAM: A solution to efficient increase the capacity of future PLC networks," *IEEE Trans. on Power Delivery*, vol. 26, no. 4, pp. 2443–2455, Oct. 2011.

[8] F. Cruz-Roldán, F. A. Pinto-Benel, J. Osés del Campo, and M. Blanco-Velasco, "A wavelet OFDM receiver for baseband power line communications," *Journal of the Franklin Institute*, vol. 353, no. 7, pp. 1654–1671.

[9] F. A. Pinto-Benel, M. Blanco-Velasco, and F. Cruz-Roldán, "Throughput analysis of wavelet OFDM in broadband power line communications," *IEEE Access*, vol. 6, pp. 16 727–16 736, 2018.

[10] "Data-over-cable service interface specifications Docsis 3.1. Physical layer specification," CM-SP-PHYv3.1-I07-150910, September 2015.

[11] "IEEE standard for broadband over power line networks: Medium access control and physical layer specifications," IEEE Std 1901-2010, December 2010.

[12] "IEEE standard for low-frequency (less than 500 khz) narrowband power line communications for smart grid applications," IEEE Std 1901.2-2013, September 2013.

[13] "Unified high-speed wireline-based home networking transceivers - system architecture and physical layer specification," ITU-T Recommendation G.9960, September 2018.

[14] "Unified high-speed wireline-based home networking transceivers – multiple input/multiple output specification," ITU-T Recommendation G.9963, November 2018.

[15] S. D'Alessandro, A. M. Tonello, and L.Lampe, "Adaptive pulse-shaped OFDM with application to in-home power line communications," *Telecommunication Systems*, vol. 51, no. 3-13, September 2012.

[16] S. H. Müller-Weinfurtner, "Optimum Nyquist windowing in OFDM receivers," *IEEE Transactions on Communications*, vol. 49, no. 3, pp. 417–420, 2001.

[17] R. Zayani, Y. Medjahdi, H. Shaiek, and D. Roviras, "WOLA-OFDM: A potential candidate for asynchronous 5G," in *2016 IEEE Globecom Workshops (GC Wkshps)*, 2016, pp. 1–5.

[18] C. An and H. Ryu, "CPW-OFDM (cyclic postfix windowing OFDM) for the B5G (beyond 5th generation) waveform," in *2018 IEEE 10th Latin-American Conference on Communications (LATINCOM)*, 2018, pp. 1–4.

[19] Y.-P. Lin, C. Li, and S.-M. Phoong, "A filterbank approach to window designs for multicarrier systems," *IEEE Circuits and Systems Magazine*, vol. 7, no. 1, pp. 19–30, 2007.

[20] A. J. Redfern, "Receiver window design for multicarrier communication systems," *IEEE Journal on Selected Areas in Communications*, vol. 20, no. 5, pp. 1029–1036, 2002.

[21] T. Weiss, J. Hillenbrand, A. Krohn, and F. K. Jondral, "Mutual interference in OFDM-based spectrum pooling systems," in *2004 IEEE 59th Vehicular Technology Conference. VTC 2004-Spring (IEEE Cat. No.04CH37514)*, vol. 4, 2004, pp. 1873–1877 Vol.4.

[22] E. Bala, J. Li, and R. Yang, "Shaping spectral leakage: A novel low-complexity transceiver architecture for cognitive radio," *IEEE Vehicular Technology Magazine*, vol. 8, no. 3, pp. 38–46, 2013.

[23] T. Nhan-Vo, K. Amis, T. Chonavel, and P. Siohan, "Achievable throughput optimization in OFDM systems in the presence of interference and its application to power line networks," *IEEE Transactions on Communications*, vol. 62, no. 5, pp. 1704–1715, May 2014.

[24] L. Díez, J. A. Cortés, F. J. Cañete, E. Martos-Naya, and S. Iranzo, "A generalized spectral shaping method for OFDM signals," *IEEE Transactions on Communications*, vol. 67, no. 5, pp. 3540–3551, 2019.

[25] B. Peköz, Z. E. Ankarali, S. Köse, and H. Arslan, "Non-redundant OFDM receiver windowing for 5G frames and beyond," *IEEE Transactions on Vehicular Technology*, vol. 69, no. 1, pp. 676–684, 2020.

[26] N. Al-Dhahir and J. M. Cioffi, "Optimum finite-length equalization for multicarrier transceivers," *IEEE Transactions on Communications*, vol. 44, no. 1, pp. 56–64, Jan. 1996.

[27] ——, "A bandwidth-optimized reduced-complexity equalized multicarrier transceiver," *IEEE Transactions on Communications*, vol. 45, no. 8, pp. 948–956, Aug. 1997.

[28] D. Kim and G. L. Stuber, "Residual ISI cancellation for OFDM with applications to HDTV broadcasting," *IEEE Journal on Selected Areas in Communications*, vol. 16, no. 8, pp. 1590–1599, Oct. 1998.

[29] G. Arslan, B. L. Evans, and S. Kiaei, "Equalization for discrete multitone transceivers to maximize bit rate," *IEEE Transactions on Signal Processing*, vol. 49, no. 12, pp. 3123–3135, Dec. 2001.

[30] K. Van Acker, "Equalization and echo cancellation for DMT-based DSL modems," Ph.D. dissertation, Katholieke Universiteit Leuven, Belgium, 2001.

[31] W. Henkel, G. Tauböck, P. Ödling, P. O. Börjesson, and N. Petersson, "The cyclic prefix of OFDM/DMT - An analysis," in *Proceedings of 2002 International Zurich Seminar on Broadband Communications. Access, Transmission, Networking*, 2002, pp. 22–1–22–3.

[32] M. Milošević, L. F. C. Pessoa, B. L. Evans, and R. Baldick, "DMT bit rate maximization with optimal time domain equalizer filter bank architecture," in *Thirty-Sixth Asilomar Conference on Signals, Systems and Computers*, vol. 1, Nov. 2002, pp. 377–382.

[33] T. Pham, T. Le-Ngoc, G. K. Woodward, and P. A. Martin, "Channel estimation and data detection for insufficient cyclic prefix MIMO-OFDM," *IEEE Transactions on Vehicular Technology*, vol. 66, no. 6, pp. 4756–4768, June 2017.

[34] B. Lim and Y. C. Ko, "SIR analysis of OFDM and GFDM waveforms with timing offset, CFO, and phase noise," *IEEE Transactions on Wireless Communications*, vol. 16, no. 10, pp. 6979–6990, Oct. 2017.

[35] W. A. Martins, F. Cruz-Roldán, M. Moonen, and P. S. R. Diniz, "Intersymbol and intercarrier interference in OFDM transmissions through highly dispersive channels," in *2019 27th European Signal Processing Conference (EUSIPCO)*, 2019, pp. 1–5.

[36] N. C. Beaulieu and P. Tan, "On the effects of receiver windowing on OFDM performance in the presence of carrier frequency offset," *IEEE Trans. on Wireless Communications*, vol. 6, no. 1, pp. 202–209, 2007.

[37] T. Pollet, H. Steendam, and M. Moeneclaey, "Performance degradation of multi-carrier systems caused by an insufficient guard interval," in *Proceedings of CWAS'97-Intern. Workshop on Copper Wire Access Systems "Bridging the Last Copper Drop"*, Budapest, Hungary, 27–29 Oct 1997, pp. 265–270.

[38] "Guidelines for evaluation of radio transmission technologies for IMT-2000," ITU, Recommendation ITU-R M.1225, 1997.

[39] 3rd Generation Partnership Project, 3GPP TS 25.101, *Technical Specification Group Radio Radio Access Network. User Equipment (UE) Radio Transmission and Reception (FDD) (Release 7)*, Sep. 2007.

[40] A. García-Armada, "SNR gap approximation for M-PSK-based bit loading," *IEEE Transactions on Wireless Communications*, vol. 5, no. 1, pp. 57–60, Jan. 2006.